Available online at www.sciencedirect.com
ScienceDirect
Journal of the European Ceramic Society 30 (2010) 29–35
www.elsevier.com/locate/jeurceramsoc

Phase composition of alumina–mullite–zirconia refractory materials

C. Zanelli *, M. Dondi, M. Raimondo, G. Guarini

CNR-ISTEC, Institute of Science and Technology for Ceramics, 48018 Faenza, Italy

Received 1 April 2009; received in revised form 15 July 2009; accepted 16 July 2009
Available online 28 August 2009

Abstract

Refractories in the Al_2O_3–SiO_2–ZrO_2 system are widely used in many applications, for ceramic rollers in particular, and are characterized by high mechanical strength, excellent thermal shock resistance, resistance to corrosion by alkaline compounds and low creep at high temperature. Their performances greatly depend on the amount and chemical composition of crystalline and glassy phases, which were investigated by quantitative XRPD (RIR–Rietveld) and XRF in order to assess the effect of various Al_2O_3/SiO_2 ratios of starting batches and different alumina particle size distributions. Refractories consist of mullite, corundum, zirconia polymorphs and a vitreous phase in largely variable amounts. The mullite percentage, unit cell parameters and composition vary with sintering temperature, being mostly influenced by the Al_2O_3/SiO_2 ratio of the batch. Its orthorhombic unit cell increased its volume from 1400 to 1500 °C, while its stoichiometry became more aluminous. The corundum stability during firing is strongly affected by the Al_2O_3/SiO_2 ratio, but not by the particle size distribution of alumina raw materials. Zirconia raw materials are involved in the high temperature reactions and about one-third of the available ZrO_2 is dissolved in the glassy phase, ensuring excellent resistance to alkali corrosion, mainly depending on the fraction of coarse alumina. The phase composition of the vitreous phase increased with sintering temperature, being over 20% when the fractions of coarse alumina in the starting batch are between 0.2 and 0.5.

Keywords: Mullite; Al_2O_3–SiO_2–ZrO_2; Corundum; Glassy phase; Refractory; XRD; Zirconia

1. Introduction

An important category of refractories in the Al_2O_3–SiO_2–ZrO_2 system is based on corundum, mullite and baddeleyite structures. It is widely utilized in forehearth, feeders, glass-melting furnaces, as plungers, tubes, channels, mantle blocks, and orifice rings.[1] These materials are extensively used as refractory rollers in fast firing kilns for the manufacture of ceramic tiles, tableware and sanitaryware.[2,3] In this sector, firing technology has undergone a rapid innovation over the last decades, and has under great pressure to reduce both energy consumption and firing times. Changes in tile size and composition of fast-fired bodies and glazes brought about the progressive rearrangement of composition and properties of ceramic rollers in order to meet ever-increasing requirements. Current expectations involve improved performance in terms of refractoriness (higher operating temperatures, up to 1300 °C), thermal shock resistance (ΔT about 1200 °C), extreme resistance to corrosion by alkaline and alkaline-earth elements (coming from contact with bodies and glazes), and creep due to increasing length of rollers (over 450 cm) and rising load of ceramic tiles (from 10 to over 20 kg/m^2).[4]

The bodies for alumina–mullite–zirconia refractories are composed of raw and calcined kaolins, alumina with different particle size distribution and zirconium compounds, including zirconia–mullite composites. Their sintering is commonly carried out in the 1400–1600 °C range with prolonged soaking times. The resulting phase composition consists of mullite, corundum, zirconia polymorphs and a vitreous phase in largely variable amounts. Several phase transformations occur during firing:

(a) decomposition of clay minerals, involving dehydroxilation of kaolinite around 500 °C and further transformation over 1000 °C into mullite and silica;
(b) quartz usually disappears over 1300 °C, being incorporated in mullite or the liquid phase;
(c) zircon tends over 1400 °C to dissociate into zirconia, which on cooling undergoes the polymorphic transformation from

* Corresponding author. Tel.: +39 0546 699718; fax: +39 0546 46381.
E-mail address: chiara.zanelli@istec.cnr.it (C. Zanelli).

0955-2219/$ – see front matter © 2009 Elsevier Ltd. All rights reserved.
doi:10.1016/j.jeurceramsoc.2009.07.016

the tetragonal to the monoclinic form, so that both phases may occur in the final product.[5–8]

Such considerable compositional variability, depending to some extent on the phase evolution with firing temperature, can significantly affect the technological properties of refractories.[9–14] For this reason, several studies have focused on the possibility of improving the performances of alumina–mullite–zirconia refractories, in particular mechanical properties, thermal shock behavior and corrosion resistance, by varying amount and particle size distribution of raw materials.[15–22] For example, by increasing the zircon amount or adding fine-grained alumina densification was improved through a significant reduction of porosity. Faster sintering was observed together with the formation of a liquid phase filling interparticle voids.[8–13]

Therefore, many technological properties of alumina–mullite–zirconia refractories greatly depend on phase composition. For example, it is expected that an increase of the mullite-to-corundum ratio will improve the thermal shock resistance, since mullite has a thermal expansion coefficient much lower than corundum. On the other hand, creep at high temperature and resistance to corrosion by alkaline compounds depend to a large extent on the amount of glassy phase and its chemical composition.[21]

At any rate, existing literature mainly deals with alumina–mullite–zirconia refractories from the technological viewpoint and the extent of phase transformations occurring during sintering is still not sufficiently known. The aim of the present paper is to bridge this gap by investigating how phase composition, as well as chemical composition of mullite and vitreous phase, may change by varying the batch formulation and firing temperature. In particular, the effect of various Al_2O_3/SiO_2 ratios and different alumina particle size distributions has been appraised by quantitative X-ray diffraction analysis.

2. Experimental procedure

Twenty-three batches suitable for industrial refractory bodies were designed in order to get a wide range of chemical compositions (especially of Al_2O_3/SiO_2 ratios) and particle size distributions (of corundum). Every body consists of kaolin (20–30%), different kinds of alumina, each with its own particle size distribution (50–60%), zirconium compounds (10–15%), and amorphous silica (<5%).

Overall, the batches plot in the Al_2O_3–SiO_2–ZrO_2 ternary diagram close to the mullite composition, being characterized by a nearly constant ZrO_2 content, but Al_2O_3 and SiO_2 amounts which vary significantly (Fig. 1). In particular, the Al_2O_3/SiO_2 ratio ranges from 3 to 6.5, while the weight fraction of coarse-grained alumina (48 mesh) on total alumina raw materials fluctuates from 0.1 and 0.6 (Fig. 2).

All ceramic bodies underwent a simulation of the industrial processing of refractory materials on a laboratory pilot line. In particular, the following working phases were carried out:

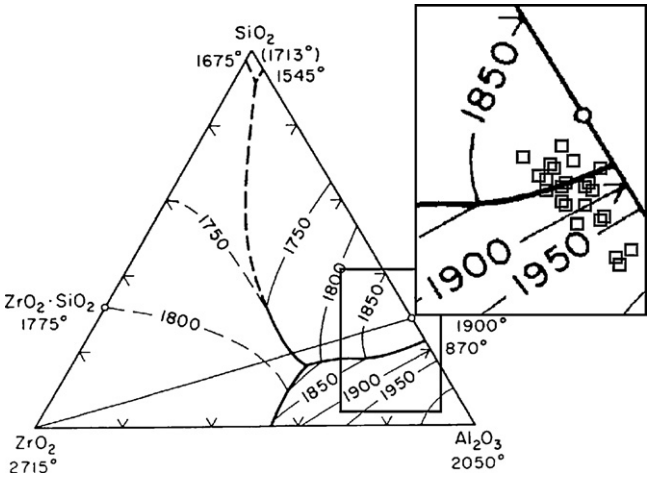

Fig. 1. Chemical composition of refractories plotted in the Al_2O_3–ZrO_2–SiO_2 diagram.

- hand mixing of raw materials and humidification with 13–15 wt.% water, then storage for 24 h;
- extrusion of 100 mm × 20 mm × 10 mm bars by means of a pneumatic apparatus;
- drying at ambient temperature for 24 h, then in electric oven at 105 ± 5 °C overnight;
- firing in an electric chamber kiln, in static air, at two different maximum temperatures (1400 and 1500 °C) with an industrial-like cycle (8 h soaking, 30 h cold-to-cold).

The fired samples were pulverized by jaw crushing (<10 mm), hammer grinding (<1 mm), and wet ball milling (<0.06 mm), then dried in oven (105 °C overnight) and disagglomerated in agate mortar. The powders were characterized by quantitative phase analysis (XRPD, Siemens D500, Cu Kα radiation, 10–80° 2θ range, scan rate 0.02° 2θ, 4 s per step). Samples were prepared adding 10 wt.% of TiO_2 (NIST 674) as internal standard and following a RIR (Reference Intensity Ratio) and the Rietveld refinement techniques,[23] using the GSAS-EXPGUI software.[24,25] Each X-ray powder diffraction pattern

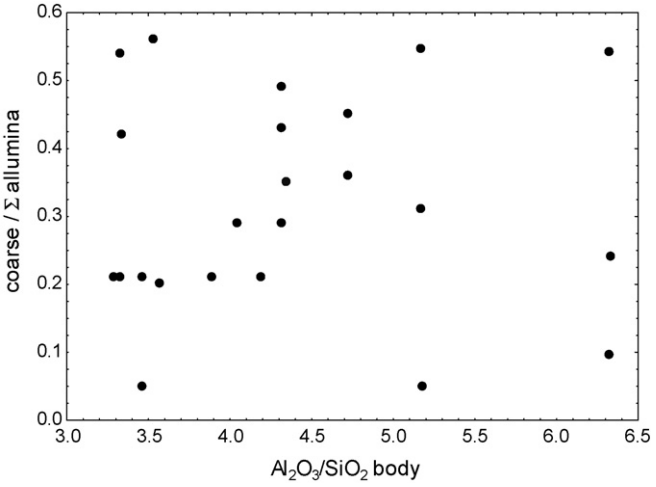

Fig. 2. Al_2O_3/SiO_2 ratios and fractions of coarse Al_2O_3 particles of the selected 23 batches.

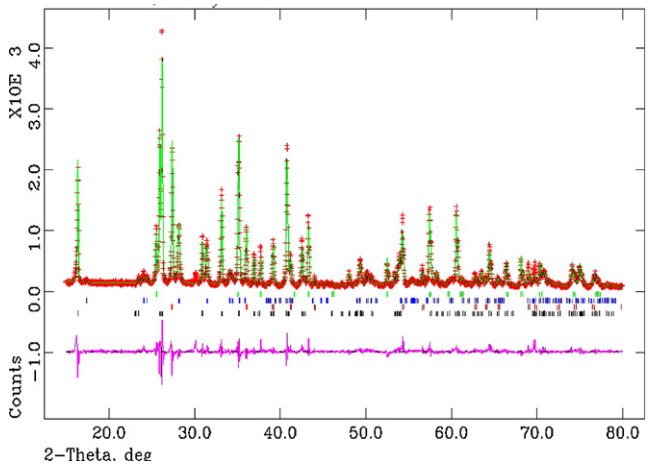

Fig. 3. Plot of Rietveld refinement performed on X-ray powder diffraction data. The experimental data are indicated by plus signs, the calculated pattern is the continuous line and the lower curve is the weighted difference between the calculated and observed patterns. The rows of vertical tick marks shows the allowed reflections for the crystalline phases present in the sample.

consists approximately of 4000 data point and 400 reflections; an example of Rietveld refinement is shown in Fig. 3. The starting structural models were taken from Ban and Okada[26] for mullite, selecting the temperatures closer to that of body firing (1400 and 1600 °C); from Oetzel and Heger[27] for corundum, for zirconia polymorphs from Wang et al.[28], and for rutile from the database NIST.[29] Up to 40 independent variables were refined: phase fractions, zero point, 15–20 coefficients of the shifted Chebyschev function to fit the background, unit cell parameters, profile coefficients (one Gaussian, G_w, and one Lorentzian term, L_x). For some samples the preferred orientation along the plane [3 3 0] of corundum was refined using the March-Dollase approximation.

The agreement indices, as defined in GSAS, for the final least-squares cycles of all refinements are represented by R_p (%), R_{wp} (%), X^2 and $R(F^2)$ (%).[25,26] For the refined patterns, they were found in the following ranges: $8.5\% < R_p < 12.5\%$, $11.0\% < R_{wp} < 15.5\%$, $3.5 < X^2 < 6.0$, and $9.5\% < R(F^2) < 13.0\%$.

The experimental uncertainty of in the quantitative determination of phases amount is within 5% relative.

The chemical composition of mullite was calculated by means of unit cell parameters on the basis of the empirical relationship between the length of the unit cell edge a and the Al_2O_3 content[27]:

$$Al_2O_3 \ (\text{mol.}\%) = 1443(\text{length of axis } a) - 1028.06$$

The chemical composition of the vitreous phase was calculated from the bulk chemistry of each batch, subtracting the individual contributions of every crystalline phase (mullite, corundum and zirconia according to their own stoichiometry) then normalizing to 100%.

In this study, the contour maps were used as a means of interpreting the phase transformations investigated, in terms of their amounts. The contour maps were obtained by the Statistica[30] software: every plot is an optimized linear interpolation from which three dimensional surfaces can be generated. The maps sort the Al_2O_3–SiO_2–ZrO_2 system by its fraction of coarse particles on the whole alumina of the batch on the ordinate and the Al_2O_3/SiO_2 ratio of the body on the abscissa. The amount of each phase at the two sintering temperatures (1400–1500 °C) is represented by color fields.

3. Results and discussion

The industrial refractories under investigation consist of mullite, corundum, zirconia (baddeleyite predominant over the tetragonal polymorph) and a vitreous phase. The most abundant phase is mullite, usually ranging from 50 to 60% after sintering at 1400 °C and rising to 60–80% after firing at 1500 °C. As observed in the literature,[5,8,31–34] increasing the mullite content, a proportional decreasing of corundum occurs, whose amount goes from 20–35% (1400 °C) down to 15–30% (1500 °C), while zirconia remains in nearly constant amount (2–6%). The glassy phase, present in relatively small amount (10–13%) at the lower sintering temperature, remarkably increases after firing at 1500 °C (15–25%).

The unit cell parameters of mullite vary in rather restricted ranges ($0.7550\ \text{nm} < a < 0.7630\ \text{nm}$, $0.7688\ \text{nm} < b < 0.7692\ \text{nm}$, $0.2884\ \text{nm} < c < 0.2887\ \text{nm}$) which correspond to the orthorhombic lattice.[26] Within these ranges, the unit cell volume increased with sintering temperature (Fig. 4), suggesting a change in the chemical composition of mullite, as expected by literature data[9,26,34–35]: the alumina content of mullite is higher after firing at 1500 °C (62–63.5% mol) than at 1400 °C (61–62% mol). The mullite stoichiometry depends also on the batch composition: increasing the Al_2O_3/SiO_2 ratio of the bodies, a progressive alumina enrichment of mullite can be observed as separate trends for the two sintering temperatures (Fig. 5) confirming previous observations.[31] On the other hand, the more abundant is mullite, the lower its alumina content, even though this variation occurs in a quite restricted range (Fig. 6). Moreover, the mullite amount seems to be basically influenced by the Al_2O_3/SiO_2 ratio of the batch, since the fields in the contour map are approximately parallel to the axis of alumina particle size distribution, which therefore does not affect significantly the mullite formation (Fig. 7).

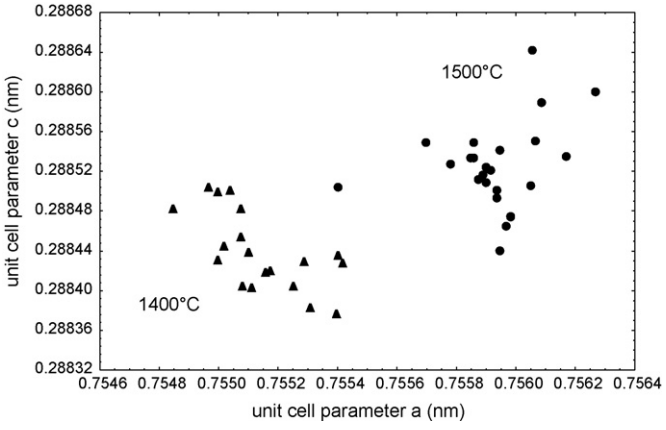

Fig. 4. Variation of mullite a and c unit cell parameters at different sintering temperatures.

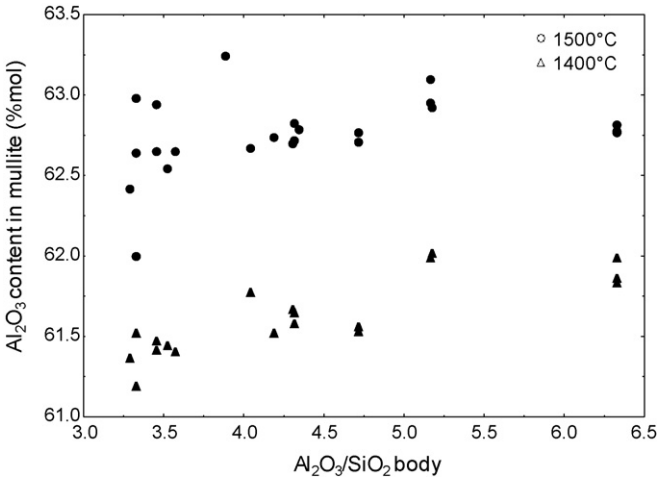

Fig. 5. Al_2O_3/SiO_2 ratio of the body vs. the alumina content of mullite.

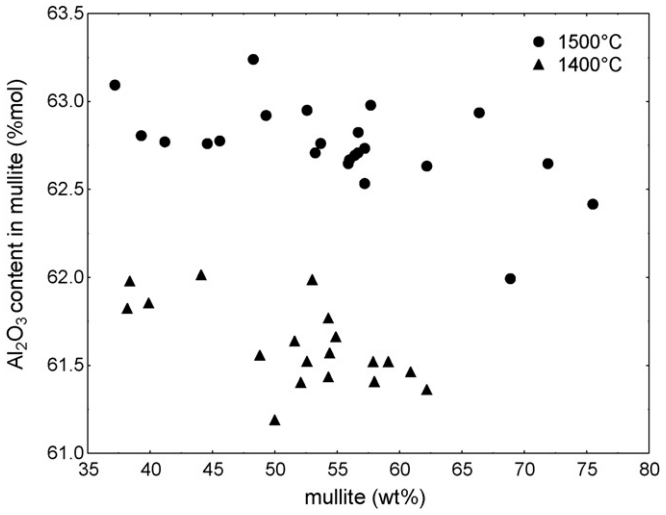

Fig. 6. Amount of mullite in the bodies vs. the alumina content of mullite.

The corundum stability during firing depends to a large extent on the Al_2O_3/SiO_2 ratio, as it can be appreciated in the contour maps (Fig. 8). The limited effect of the particle size of alumina raw materials on the final corundum content is somehow unexpected.

During sintering, mullite–corundum–zirconia refractories undergo a complex chemical balance, involving not only the phase amounts, but also the composition of mullite and vitreous phase. In fact, the glass formed in the 1400–1500 °C range

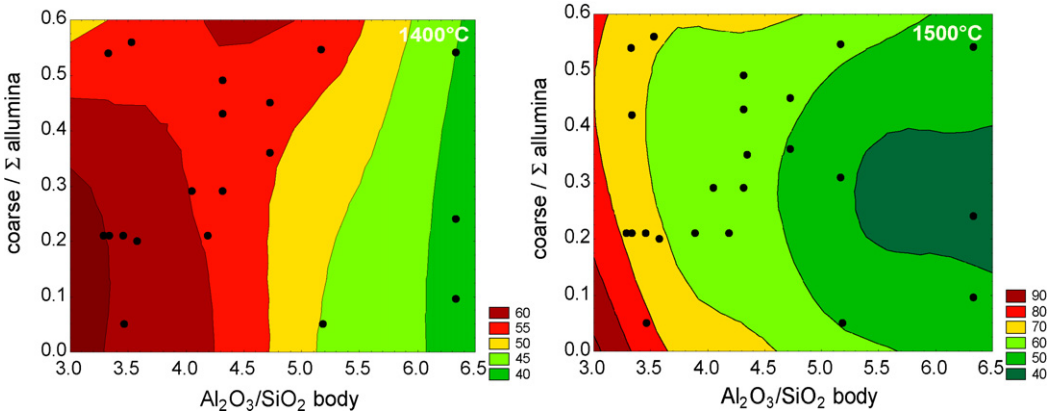

Fig. 7. Contour maps of mullite amount (wt.%) at two sintering temperatures (1400–1500 °C) as function of the Al_2O_3/SiO_2 ratio of the body and the fraction of coarse particles (48 mesh) on the total raw alumina of the batch (coarse/Σalumina). ()

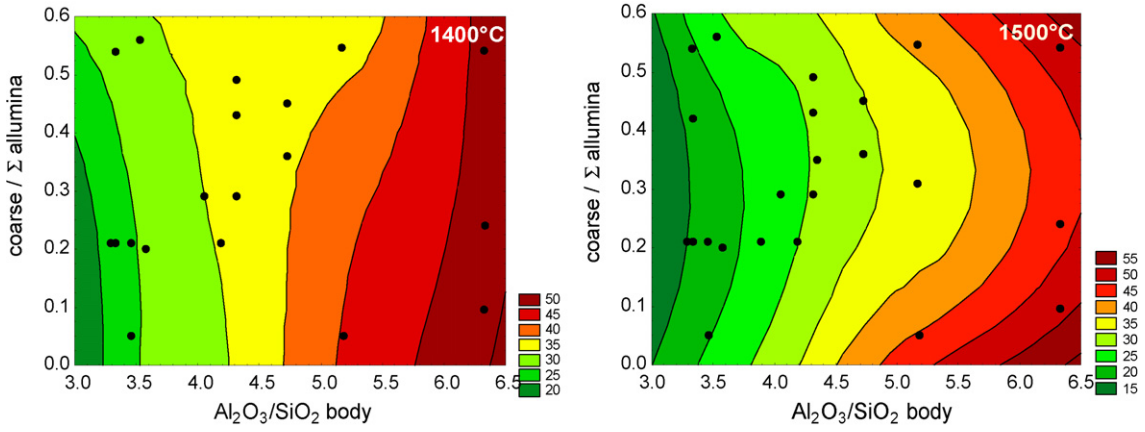

Fig. 8. Contour maps of corundum amount (wt.%) at two sintering temperatures (1400–1500 °C) in function of the Al_2O_3/SiO_2 ratio of the body and the fraction of coarse particles (48 mesh) on the total raw alumina of the batch (coarse/Σalumina). (For interpretation of the references to color in this figure legend, the reader is referred to the web version of the article.)

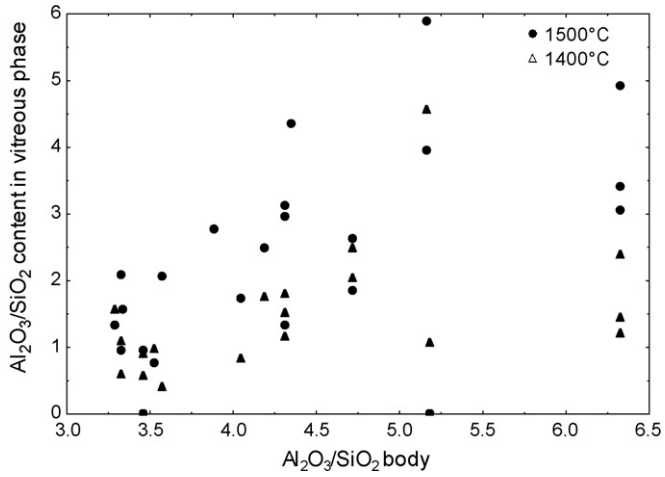

Fig. 9. Relation between the Al_2O_3/SiO_2 content in the vitreous phase and the Al_2O_3/SiO_2 ratio of the mixture.

exhibits a wide compositional spectrum, varying in terms of Al_2O_3/SiO_2 ratio from below 0.5 to about 6 at both sintering temperatures, following to some extent the fluctuations of the Al_2O_3/SiO_2 ratio of the batch (Fig. 9). Such compositional range is different and much wider than previously observed in the literature[36] and might account for different behavior (e.g. resistance to alkali attack, creep).

The amount of residual zirconia is not significantly affected by sintering temperature, being always in the 2–6% range. However, it is mainly influenced by the particle size distribution of raw alumina, as shown in the contour maps (Fig. 10); zirconia appears to be more stable when the fraction of coarse alumina is either very abundant (>0.5) or scarce (<0.2). Interestingly, the vitreous phase contains a relatively large amount of zirconia, corresponding approximately to one-third of total ZrO_2 of the batch. This fact is able to explain the excellent resistance to alkali corrosion of mullite–corundum–zirconia refractories, besides their relatively high content of glassy phase.[10,21]

These chemical compositions of the glassy phase plot in the ternary diagram Al_2O_3–SiO_2–ZrO_2 at liquidus temperatures

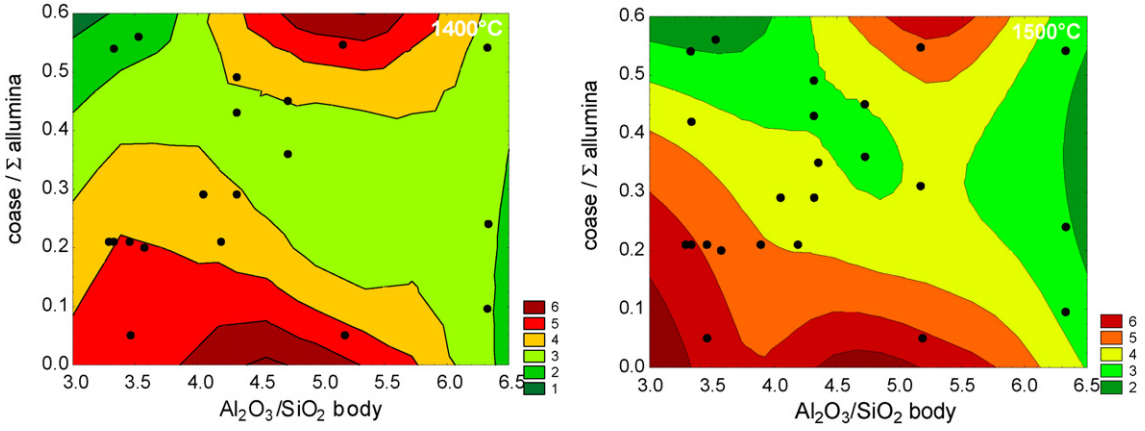

Fig. 10. Contour maps of zirconia amount (wt.%) at two sintering temperatures (1400–1500 °C) in function of the Al_2O_3/SiO_2 ratio of the body and the fraction of coarse particles (48 mesh) on the total raw alumina of the batch (coarse/Σalumina). (For interpretation of the references to color in this figure legend, the reader is referred to the web version of the article.)

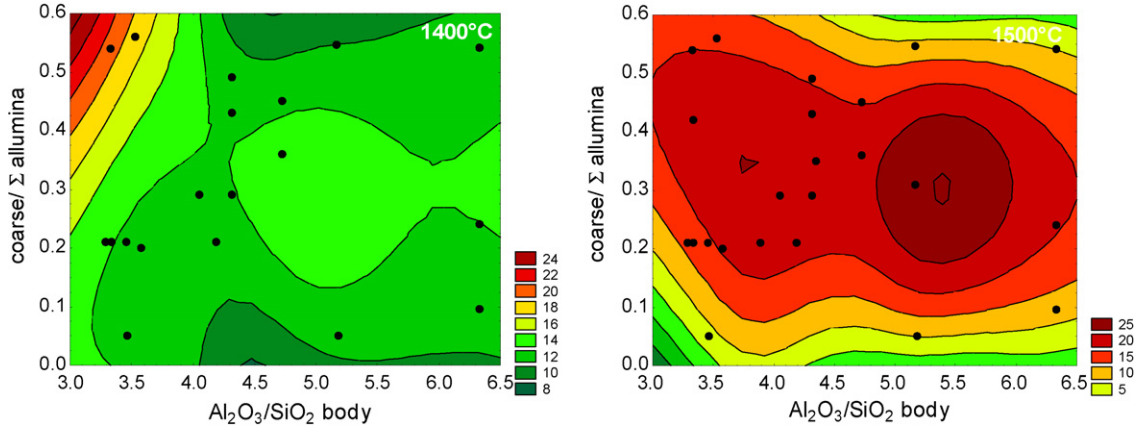

Fig. 11. Contour maps of vitreous phase amount (wt.%) at two sintering temperatures (1400–1500 °C) in function of the Al_2O_3/SiO_2 ratio of the body and the fraction of coarse particles (48 mesh) on the total raw alumina of the batch (coarse/Σalumina). (For interpretation of the references to color in this figure legend, the reader is referred to the web version of the article.)

between 1750 and 1850 °C, i.e. well above the actual sintering temperatures. Therefore, the role played by impurities, mainly supplied by kaolin, which tend to concentrate in the liquid phase, lowering significantly the melting temperature is important. The amount of these impurities in the glassy phase is estimated to be in the following ranges: 0.3–0.5% for Fe_2O_3, 0.2–0.5% for TiO_2, 0.1–0.3% for alkaline-earth elements and 0.1–0.4% for alkalis.

A key factor affecting phase equilibria in the mullite–corundum– zirconia refractories segment of the Al_2O_3–SiO_2–ZrO_2 system seems to be the amount of silica available. The amount of mullite tends to grow up to the maximum permitted by the SiO_2 content of the batch. Such increasing is stressed at expenses of the glassy phase, since the mullite composition moves towards a term richer in alumina.

The amount of vitreous phase at 1400 °C is in a narrow range (10– 15%) while at 1500 °C it reaches in practically up to 30% for the values of all samples (Fig. 11). The contour maps show that the formation of vitreous phase does not depend on the Al_2O_3/SiO_2 ratio, but mainly on the particle size distribution of raw alumina: fractions of coarse alumina between 0.2 and 0.5 ensure the formation of over 20% liquid phase during sintering.

4. Conclusions

Detailed knowledge of phase transformations occurring during firing is fundamental in the design of alumina–mullite–zirconia refractories with optimized technological properties. Their phase composition consists of mullite, corundum, zirconia and a vitreous phase. The amount and chemical composition of these phases vary depending on the firing temperature, the Al_2O_3/SiO_2 ratio of the batches and the particle size distribution of alumina raw materials.

Mullite changes its amount, unit cell parameters and composition with firing temperature, being mostly influenced by the Al_2O_3/SiO_2 ratio of the batch. Its structure is of the orthorhombic type, and undergoes an increase in its unit cell volume from 1400 to 1500 °C, while its stoichiometry turns to terms richer in alumina.

The extent of corundum reaction during firing depends on the Al_2O_3/SiO_2 ratio of the batches, but it is unexpectedly not significantly influenced by the particle size distribution of alumina raw materials.

Zirconia raw materials are involved in the high temperature reactions and about one-third of the available ZrO_2 is dissolved, probably giving the glassy phase its excellent resistance to alkali corrosion. Baddeleyite predominantes over tetragonal zirconia and their amount is mainly influenced by the particle size distribution of raw alumina.

The vitreous phase tends to increase with sintering temperature, but the formation of over 20% liquid phase occurs with intermediate fractions of coarse alumina in the starting batch (0.2–0.5). For the first time, an extensive chemical characterization of the vitreous phase has been accomplished for mullite–corundum–zirconia refractories.

References

1. Aksel, C., Mechanical properties and thermal shock behaviour of alumina–mullite–zirconia and alumina–mullite refractory materials by slip casting. *Ceram. Int.*, 2003, **29**, 311–316.
2. Sonntag, U., Variety of ceramic roller materials: answer to increased requirements of new applications and developments. *Interceram*, 2001, **50**, 380–387.
3. Bettges, H., High-alumina rollers for rollers kilns. *Interceram*, 1990, **39**, 28–30.
4. Sonntag, U., Isenmann, B., Knape, G., Sussmuth, M. and Habermann, A., New roller concepts for extreme applications. *Proc. Eng.*, 2002, **79**, 22–26.
5. Mazzei, A. C. and Rodrigues, J. A., Alumina–mullite–zirconia composites obtained by reaction sintering. Part I. Microstructure and mechanical behaviour. *J. Mater. Sci.*, 2000, **35**, 2807–2814.
6. Mazzei, A. C. and Rodrigues, J. A., Alumina–mullite–zirconia composites obtained by reaction sintering. Part II. R-Curve behavior. *J. Mater. Sci.*, 2000, **35**, 2815–2824.
7. Lee, W. E., Argent, B. and Zhang, S., Complex phase equilibria in refractories design and use. *J. Am. Ceram. Soc.*, 2002, **85**, 2911–2918.
8. Ebadzadeh, T., Reaction sintering of multicomponent mixtures for producing ceramics containing zirconia. *J. Eur. Ceram. Soc.*, 2000, **20**, 725–729.
9. Koyama, T., Hayashi, S., Yasumori, A., Okada, K., Schmucker, M. and Schneider, H., Microstructure and mechanical properties of mullite/zirconia composites prepared from alumina and zircon under various firing conditions. *J. Eur. Ceram. Soc.*, 1996, **16**, 231–237.
10. Valle, M., Gandolfi, S., Dondi, M. and Fabbri, B., Effectiveness of various zirconium compounds in the body to improve the alkaline attack resistance of ceramic rollers. In *Fourth Euro-Ceramics*, vol. 13, 1995, pp. 131–136.
11. Aksel, C., The influence of zircon on the mechanical properties and thermal shock behaviour of slip-cast alumina–mullite refractories. *Mater. Lett.*, 2002, **57**, 992–997.
12. Aksel, C., The role of fine alumina and mullute particles on the thermomechanical behaviour of alumina–mullite refractory materials. *Mater. Lett.*, 2002, **57**, 708–714.
13. Aksel, C., Dexet, M., Logen, N., Porte, F., Riley, F. L. and Konieczny, F., The influence of zircon in a model aluminosilicate glass tank forehearth refractory. *J. Eur. Ceram. Soc.*, 2003, **23**, 2083–2088.
14. Aksel, C., The effect of mullite on the mechanical properties and thermal shock behaviour of alumina–mullite refractory materials. *Ceram. Int.*, 2003, **29**, 183–188.
15. Valle, M., Gandolfi, S., Dondi, M. and Fabbri, B., Determination of thermal shock resistance in ceramic rollers. In *Fourth Euro-Ceramics*, vol. 3, 1995, pp. 465–470.
16. Başpinar, M. S., Schulle, W. and Kara, F., Fundamental for optimization of binding for high refractory mullite products. *Key Eng. Mater.*, 2004, **264–268**, 1787–1790.
17. Collini, M. and Rowcliffe, D., Analysis and prediction of thermal shock in brittle materials. *Acta Mater.*, 2000, **48**, 1655–1665.
18. Wang, G. and Krstic, V., Roles of porosity, residual stresses and grain size in the fracture of brittle solids. *Philos. Mag. A*, 1998, **78**(5), 1125–1135.
19. Aksel, C., Mechanical properties of alumina–mullite–zircon refractories. *Key Eng. Mater.*, 2004, **264–268**, 1791–1794.
20. Aksel, C., The influence of fine alumina particles on the mechanical properties and thermal shock behaviour of slip-cast alumina–mullite refractories. *Key Eng. Mater.*, 2004, **264–268**, 1811–1814.
21. Aksel, C., Riley, F. L. and Konieczny, F., The corrosion resistance of alumina–mullite–zircon refractories in molten glass. *Key Eng. Mater.*, 2004, **264–268**, 1803–1806.
22. Takatak, Ş., Artir, R., Yilmaz, Ş. and Bindal, C., Fracture toughness of alumina–mullite composites produced by infiltration process. *Key Eng. Mater.*, 2004, **264–268**, 981–984.
23. Gualtieri, A. F., Accuracy of XRPD QPA using the combined Rietveld–RIR method. *J. Appl. Cryst.*, 2000, **33**, 267–278.
24. Larson, A. C. and Von Dreele, R. B., General structure analysis system (GSAS). In *Los Alamos National Laboratory Report LAUR*, 2000, pp. 86–748.

25. Toby, B. H., EXPGUI, a graphical user interface for GSAS. *J. Appl. Cryst.*, 2001, **34**, 210–221.
26. Ban, T. and Okada, K., Structure refinement of mullite by the Rietveld method and a new method for estimation of chemical composition. *J. Am. Ceram. Soc.*, 1992, **75**, 227–230.
27. Oetzel, M. and Heger, G., Laboratory X-ray powder diffraction: a comparison of different geometries with special attention to the usage of the CuK alpha doublet. *J. Appl. Cryst.*, 1999, **32**, 799–807.
28. Wang, D., Guo, Y., Liang, K. and Tao, K., Crystal structure of zirconia by Rietveld refinement. *Sci. China*, 1999, **42**, 80–86.
29. SRM 674b, Standard Reference Materials. In *X-Ray Powder Diffraction Intensity Set for Quantitative Analysis by X-Ray Powder Diffraction*. National Institute of Standards & Technology, Gaithersburg, USA, 2005.
30. *STATISTICA 7.1*. StatSoft Italia s.r.l., 2005.
31. Madsen, I. C., Finney, R. J., Flann, R. C. A., Frost, M. T. and Wilson, B. W., Quantitative analysis of high-alumina refractories using X-ray powder diffraction data and the Rietveld method. *J. Am. Ceram. Soc.*, 1991, **74**, 619–624.
32. Rupo, E. D. and Anseu, M. R., Solid state reactions in the $ZrO_2{\cdot}SiO_2$–αAl_2O_3 system. *J. Mater. Sci.*, 1980, **15**, 114–118.
33. Duran, C. and Tur, Y. K., Phase formation and texture development in mullite/zirconia composites fabricated by templated grain growth. *J. Mater. Sci.*, 2006, **41**, 3303–3313.
34. Zhao, S., Haung, Y., Wang, C., Haung, X. and Guo, J., Mullite formation from reaction sintering of $ZrSiO_4$/α-Al_2O_3 mixtures. *Mater. Lett.*, 2003, **57**, 1716–1722.
35. Cameron, W. E., Composition and cell dimension of mullite. *Ceram. Bull.*, 1977, **56**, 1003–1011.
36. Aksel, C., The microstructural features of an alumina–mullite–zirconia refractory material corroded by molten glass. *Ceram. Int.*, 2003, **29**, 305–309.